Response of a ring-down cavity to an arbitrary excitation

Joseph T. Hodges, J. Patrick Looney, and Roger D. van Zee
Chemical Science and Technology Laboratory, National Institute of Standards and Technology, Gaithersburg, Maryland 20899

An eigenmode analysis of the response of an empty ring-down cavity to an arbitrary laser excitation is presented. By explicitly taking into account both the mode structure of the ring-down cavity and the spectral content of the laser pulse, it is found that the complicated ring-down signals commonly observed in the laboratory can be interpreted in terms of cavity mode beating. Some conclusions drawn from this analysis are verified experimentally by measurements of the time and frequency response of empty cavities. These observations provide clear evidence for the existence of longitudinal and transverse mode structures in ring-down cavities.

I. INTRODUCTION

Many industrial processes are prone to reduced product yields and increased product defects as a consequence of trace-level gaseous contaminants. In such applications, there is a critical need for sensitive and accurate real-time monitors of contaminant concentrations. This need has driven the demand for standards-grade measurements of low level gaseous contaminants, most notably water. In response to this demand, we are exploring experimental techniques based on cavity ring-down spectroscopy (CRDS)[1–6] as the basis for new density measurement standards in vacuum environments and process gas streams.

Although CRDS is considered to be one of the most promising spectroscopic tools for quantitative measurements of rarified species,[7] its full potential has not yet been realized. Toward this end, we are investigating some of the factors that limit quantitative, CRDS-based absorbance measurements. For example, as delineated by Zalicki and Zare[3] and demonstrated in our laboratory,[8] finite linewidth effects tend to make the characteristic light amplitude decay nonexponential when the excitation laser is tuned to an absorption feature, and this in turn leads to an underestimation of the absorptive losses. In this paper we investigate the details of the complex temporal structure of ring-down signals commonly observed in the laboratory. Measured ring-down signals usually possess a great deal of periodic, high frequency structure superimposed on the overall decay signal, and this structure varies from shot-to-shot. Clearly, for the ultimate potential of CRDS as a quantitative spectroscopic technique to be realized, it is necessary to have a detailed understanding of the physical mechanisms that give rise to these complexities. In particular, the present work is motivated by the lack of a clear understanding of how the details of the construction of ring-down cavities and the characteristics of the excitation laser such as laser bandwidth and laser temporal coherence affect the temporal structure of ring-down signals.

The present work is also motivated by conflicting claims regarding the frequency selecting nature of ring-down cavities under pulsed excitation. In a recent paper by Zalicki and Zare,[3] an analysis of ring-down cavities within the framework of Fabry–Perot theory was presented. Their simulations predicted that the energy transmitted by the ring-down cavity as a function of laser detuning is not constant for certain experimental configurations. Under such conditions, Zalicki and Zare concluded that entire absorption features could be missing from spectra measured with CRDS if these features occurred at unpropitious frequencies. Subsequently, Scherer *et al.*[9] reported a series of experiments intended to test these predictions. They claimed that results of their experiments demonstrated a failure of the analysis of Zalicki and Zare and further conjectured that ring-down cavities are frequency selective only when the coherence length of the excitation is long relative to the round-trip cavity length. In response to those experiments, Lehmann and Romanini[10] presented a general framework, based on the superposition principle, for describing the excitation and response of ring-down cavities. They demonstrated that ring-down cavities act as frequency filters regardless of the temporal profile of the input field as long as the cavity ring-down time is long compared to other relevant time scales, such as the dephasing time of the absorbing species.

Here we present an eigenmode analysis of the empty ring-down cavity response that is based on the well-established theory of stable resonators. By examining in detail the eigenmode decomposition of the cavity fields, we explicitly analyze the time and frequency response of an empty ring-down cavity. The general case of cavity excitation by an arbitrary laser pulse is presented, and the specific case of cavity excitation by a frequency modulated (''chirped'') Gaussian pulse is examined in detail. Following this analysis, we present the results of experiments designed to verify specific predictions of the model. The goal is to investigate the validity of a stable resonator description of ring-down cavities injected with pulsed laser light. We find that the experimental results are consistent with predictions obtained from the stable resonator framework, and we believe this viewpoint also can explain the results of Scherer *et al.*[9]

II. RESPONSE OF A RING-DOWN CAVITY TO AN ARBITRARY EXCITATION

We consider the case of an open, axisymmetric stable resonator[11–13] constructed from two identical mirrors of finite intensity reflectivity R and radius of curvature r that are separated by a distance l. The origin of the Cartesian coordinate system is defined to be at the center of the cavity and the z axis is coincident with the cavity axis. We denote

$$E_i(x,y,z,t)=e_i(t)u_i(x,y,z)\exp(-i\omega_c t) \tag{1}$$

to be the time-domain complex analytic representation[14] of a linearly polarized input laser field, where ω_c is the laser carrier angular frequency, $u_i(x,y,z)$ specifies the transverse profile and direction of propagation of the pulse, and

$$e_i(t)=A_i(t)\exp[i\Phi_i(t)] \tag{2}$$

describes the pulse envelope and the associated phase variation with time, t. The instantaneous angular frequency of the field, ω, is given by[15]

$$\omega=\omega_c-\frac{d\Phi_i(t)}{dt}. \tag{3}$$

The spectrum of the incident (excitation) field, $\tilde{e}_i(\omega)$, is found via Fourier transformation of $e_i(t)$ and has the general form[14]

$$\tilde{e}_i(\omega)=a_i(\omega-\omega_c)\exp[i\phi_i(\omega-\omega_c)], \tag{4}$$

where $a_i(\omega-\omega_c)$ and $\phi_i(\omega-\omega_c)$ are the spectral amplitude and phase of the field, respectively. The power spectrum of the incident laser pulse is given by the modulus squared of the spectral amplitude and is peaked at ω_c. For transform-limited pulses, $\phi_i(\omega-\omega_c)$ is a constant, ϕ_0.

The cavity eigenmodes of an open resonator or cavity constitute sourceless configurations of the electromagnetic field that satisfy Maxwell's relations and the boundary conditions imposed by the mirrors.[12,16] These modes are uniquely denoted by the label, TEM_{qmn}, for the Gauss–Hermite polynomials of order (m,n) or, TEM_{qpl} for the Gauss–Laguerre polynomials of order (p,l). The (m,n) and (p,l) indices represent the number of nodes of the transverse electromagnetic field (the "transverse mode"), and the index q index is the number of nodes of the axial standing wave along the cavity axis (the "longitudinal mode"). The eigenfrequencies, ν_{qmn}, of an empty resonator are given by[12,13]

$$\nu_{qmn}=\frac{\omega_{qmn}}{2\pi}=\frac{c}{2l}\left[q+\frac{2}{\pi}\arctan\left(\frac{l}{\sqrt{l(2r-l)}}\right)(m+n+1)\right], \tag{5}$$

where c is the speed of light. The eigenfrequency associated with mode TEM_{qpl} can be found by associating $2p+l$ with $m+n$. Adjacent longitudinal modes $(\Delta q=1)$ with identical transverse mode indices are separated by the cavity free spectral range, $\omega_f/2\pi=\nu_f=c/2l$, and adjacent transverse modes $[\Delta q=0$ and $\Delta(m+n)=1]$ are separated by $\nu_{tr}=(c/\pi l)\arctan[l/\sqrt{l(2r-l)}]$. The relative values of r and l determine the transverse mode spacing, and as Eq. (5) illustrates, for fixed r the more disparate r and l, the smaller the separation is between transverse modes in comparison to the longitudinal mode spacing. A maximum separation of $\nu_{tr}=\nu_f$ occurs in a concentric resonator, for which $l=2r$. In general, transverse and longitudinal modes are not degenerate, and there is essentially a continuum of modes. However, for a fixed r there are certain cavity lengths for which the ratio of the longitudinal-to-transverse mode spacing, ν_f/ν_{tr}, is integer-valued (termed a "magic" number).[17] We exploit this degeneracy feature for such "magic" number cavities in the experiments described below. Meijers *et al.*[18] and Lehmann and Romanini[10] have previously discussed these points in the context of CRDS.

Each cavity eigenmode will be excited to varying extent depending on the overlap of the spectral content of the incident field with the cavity eigenfrequency structure and to the extent to which the transverse profile of the incident beam overlaps with the cavity transverse eigenmodes. The net field in the cavity is simply a weighted sum of all of the excited eigenmodes. Using the Gauss–Hermite polynomials,[19] $\psi_{mn}(x,y,z)$, as the basis set, the total field can be written as

$$\tilde{E}(x,y,z,\omega)=\sum_q\sum_{mn}C_{mn}\psi_{mn}(x,y,z)\tilde{e}_{qmn}(\omega), \tag{6}$$

where C_{mn} are the spatial coupling coefficients given by[19–22]

$$C_{mn}=\int_{-\infty}^{\infty}\int_{-\infty}^{\infty}u_i(x,y,-l/2)\psi_{mn}^*(x,y,-l/2)\,dx\,dy. \tag{7}$$

The associated time evolution, $E(x,y,z,t)$, is found via Fourier transformation of Eq. (6).

The frequency coupling is expressed through the complex optical transfer or response function, $\tilde{\mathscr{H}}_{qmn}(\omega)$, which relates the output field spectrum of mode (q,m,n) to the input spectrum[15]

$$\tilde{e}_{qmn}(\omega)=\tilde{\mathscr{H}}_{qmn}(\omega)\tilde{e}_i(\omega). \tag{8}$$

For the stable resonators considered herein, the total response function is the usual Fabry–Pérot response function given by[23]

$$\tilde{\mathscr{H}}_{mn}(\omega)=\frac{\mathscr{L}_{mn}}{1-(1-\mathscr{L}_{mn})\cdot\exp[i(\omega-\omega_{qmn})t_r]}, \tag{9}$$

where $\mathscr{L}_{mn}$ is the total resonator intensity loss per pass. This response function, which depends on properties of the cavity, represents the total response at frequency ω from all of the longitudinal cavity modes associated with a given transverse mode. It can be written as the summation over all individual longitudinal cavity mode response functions for transverse mode (m,n)[24,25]

$$\begin{aligned}\tilde{\mathscr{H}}_{mn}(\omega)&=\sum_q\tilde{\mathscr{H}}_{qmn}(\omega)\\&=\frac{-2}{\ln(1-\mathscr{L}_{mn})(2-\mathscr{L}_{mn})}\sum_{\Delta q=-\infty}^{\infty}\Gamma_{mn}^2\\&\quad\times\left\{\frac{1-(1-\mathscr{L}_{mn})\cdot\exp[(i\omega-\omega_{qmn}-\Delta q\,\omega_f)t_r]}{\Gamma_{mn}^2+(\omega-\omega_{qmn}-\Delta q\,\omega_f)^2}\right\},\end{aligned} \tag{10}$$

where Γ_{mn} is the cavity linewidth and $t_r = 2l/c$ is the cavity round-trip time. For frequencies close to the resonance, $|(\omega - \omega_{qmn})|t_r \ll 1$ and for small losses such that $\mathscr{L}_{mn} \ll 1$, the individual mode response functions of Eq. (10) are closely approximated by the familiar dispersion function,

$$\tilde{\mathscr{H}}_{qmn}(\omega) \approx \frac{\Gamma_{mn}}{\Gamma_{mn} - i(\omega - \omega_{qmn})}. \tag{11}$$

This approximate decomposition of the total cavity response function into the sum of dispersion functions facilitates in the eigenmode decomposition of the total field exiting the cavity.

The finite cavity linewidth arises from losses in the resonator such as the finite reflectivity of the mirrors and transverse mode-dependent diffraction losses. The linewidth, the intensity decay constant, τ_{mn}, and the intensity loss per pass are all related through,

$$\Gamma_{mn} = \frac{1}{2\tau_{mn}} = \frac{-\ln(1 - \mathscr{L}_{mn})}{t_r}. \tag{12}$$

For mirrors of intensity reflectivity R, and diffraction losses $\mathscr{L}_{mn}^{\text{diff}}$, the total loss per pass is given by

$$\mathscr{L}_{mn} = 1 - R + \mathscr{L}_{mn}^{\text{diff}}. \tag{13}$$

Here $1-R$ includes the losses in the dielectric mirror coating and mirror substrate that are associated with absorption, scattering, and transmission of the light. The phase shifts in the reflected field due to these weakly frequency-dependent absorption and scattering processes are expected to be small and have been neglected in this discussion.

An important figure of merit for an open resonator is the effective Fresnel number, N_F, which represents the ratio of the angle subtended by one mirror to the angle of diffraction of the electromagnetic wave as it travels across the cavity. This determines $\mathscr{L}_{mn}^{\text{diff}}$ and in turn the maximum mode order sustainable in a cavity,[26] which is of the order of πN_F. For a particular transverse mode,[27–30] the diffraction losses decrease exponentially with increasing N_F. As a typical example, consider a 50 cm long ring-down cavity constructed from 1 cm diameter mirrors with $1-R = 10^{-4}$ and $r = 100$ cm. For this cavity, $N_F \approx 20$, and in this case, $\mathscr{L}_{mn}^{\text{diff}} \sim 10^{-4}$ only when $m+n \sim 46$. Thus, only very high order modes have diffraction losses comparable with those associated with the finite mirror reflectivity.

The excitation of the transverse modes is governed by the overlap integral, Eq. (7). Its structure implies that on-axis injection of an axisymmetric beam will excite, to a varying extent, all even-order modes of the cavity unless perfect mode matching is achieved.[20,22] In practice, transverse mode matching is not ensured without careful measurements of the spatial structure of the light exiting the cavity. On the other hand, light injected off-axis will excite, to a varying extent, both even- and odd-order cavity eigenmodes. Since the classical optics ray trajectories within cavities can be cast in terms of a linear superposition of cavity transverse eigenmodes,[31] the propagation of light within a cavity along off-axis paths implies the excitation of many transverse modes. Furthermore, despite claims to the contrary,[6] the cavity eigenmodes do not "walk" around the cavity exit plane, since the ψ_{mn}'s are time independent. However, since the total field is expressed as a linear superposition of the eigenmode terms, it can assume a complicated space and time dependence which describes ray propagation within the cavity.[32,33]

Using Eq. (8), along with Eqs. (4) and (11), one can calculate the total field exiting the cavity, given by Eq. (6). After Fourier transformation to obtain the time-domain representation of the total field, we can derive an expression for the radiant flux transmitted through the end mirror of the cavity (signal), $\dot{\mathscr{E}}(t)$. In the limit that both the amplitude and phase variations in the excitation spectrum are broad relative to the width of the cavity modes, we find

$$\begin{aligned}\dot{\mathscr{E}}(t) = 2\sqrt{\epsilon_0/\mu_0} \sum_{qmn} \sum_{q'm'n'} & a_i(\omega_{qmn} - \omega_c) a_i(\omega_{q'm'n'} - \omega_c) \\ & \times \Gamma_{qmn}\Gamma_{q'm'n'} \exp(-\Gamma_{qmn}t) \exp(-\Gamma_{q'm'n'}t) \\ & \times \cos[(\omega_{qmn} - \omega_{q'm'n'})t + \phi_i(\omega_{qmn} - \omega_c) \\ & - \phi_i(\omega_{q'm'n'} - \omega_c)] \cdot C_{mn} C^*_{m'n'} \\ & \times \int\int \psi_{mn}(x,y,l/2)\psi^*_{m'n'}(x,y,l/2)\, dx\, dy,\end{aligned} \tag{14}$$

where ϵ_0 and μ_0 are the permittivity and permeability of free space, respectively.

This expression describes the time evolution of the output signal arising from radiation from the excited cavity modes, but assumes an instantaneous cavity response at $t=0$. It is in general valid for times greater than the input laser's pulse duration and shows that the output signal is a sum of weighted exponential decays modulated by sinusoidal beats whose frequencies correspond to the cavity eigenfrequency spacings. Although this expression describes beating between all excited modes, transverse mode beating will be observed only if the orthogonality between transverse modes is not preserved, such as when part of the detector is obscured, when the detector has a nonuniform response, or when there are inhomogeneous losses in the output coupling optics. This expression also accounts for the effect of temporal incoherence in the input laser field through the variation in the phase of the input spectrum.

One can calculate the complete ring-down signal, including the transient response of the cavity using the response function of the cavity, Eq. (9), and numerical Fourier transformation of Eq. (6). The result of such a computation for the single mode excitation of a 13.4 cm long cavity ($\upsilon_f = 1.12$ GHz, $\mathscr{L}_{mn} = 0.002$/pass) by a transform-limited Gaussian pulse ($\Delta\nu_{\text{FWHM}} = 93$ MHz, $\Delta t_{\text{FWHM}} = 4.80$ ns) is given in Fig. 1. In this calculation, the laser carrier frequency was detuned from the nearest cavity eigenfrequency by 100 MHz. The transient response of the cavity exhibits a sharp spike near $t=0$, and this transient is completely over in ~3 laser pulse widths (~15 ns). After that time, the output is the single exponential decay precisely predicted by Eq. (14). Use of Eq. (11) in lieu of Eq. (9) for the response function gives nearly indistinguishable results, indicating that the dispersion function is an excellent approximation to $\mathscr{H}_{qmn}(\omega)$ for this

case. Other calculations demonstrate that for a given excitation the transient spike does not change with detuning of the laser, and that the variation in the amplitude of the exponentially decaying signal is precisely as predicted by Eq. (14). For zero detuning, the amplitude of this spike and the exponential signal are equal. Also shown in Fig. 1 is the calculated temporal variation of the instantaneous frequency [Eq. (3)] of the exiting field. As is evident from this figure, the instantaneous frequency of the output field chirps from the laser carrier frequency to the nearest cavity eigenfrequency during the transient portion of the cavity's response. This result demonstrates that the ring-down signal contains information only about the optical losses at the cavity eigenfrequencies. Finally, from these simulations we find that Eq. (14) contains all the information about the decay signal that is of interest in CRDS.

Another measurable quantity is the energy transmitted by the cavity as a function of laser carrier frequency, $\mathscr{E}(\omega_c)$. We define the cavity transmittance, $\mathscr{T}(\omega_c)$, to be, $\mathscr{E}(\omega_c)/\mathscr{E}_p$, where $\mathscr{E}_p$ is the incident pulse energy. This is calculated by taking the modulus squared of the total exiting field given by Eq. (6), integrating over the exit plane of the cavity, and integrating over all frequencies. [Note that the summation over the longitudinal mode index, q, yields the total cavity response function of transverse mode (m,n) operating on the input excitation spectrum.] The resulting transmittance, valid for an arbitrary input field, is

$$\mathscr{T}(\omega_c)=\frac{1}{\mathscr{E}_p}\int_0^\infty \frac{\sqrt{\epsilon_0/\mu_0}}{\pi}\sum_{mn}|C_{mn}|^2 \times\frac{\mathscr{S}_{mn}^2|a_i(\omega-\omega_c)|^2}{1+(1-\mathscr{S}_{mn})^2-2(1-\mathscr{S}_{mn})\cdot\cos[(\omega-\omega_{qmn})t_r]}\,d\omega. \tag{15}$$

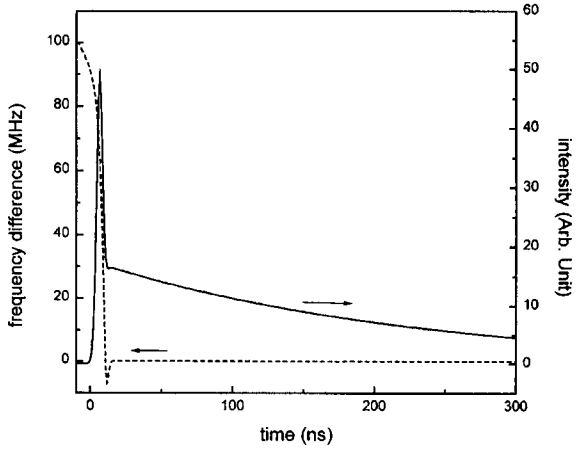

FIG. 1. Calculated ring-down signal (solid line) and instantaneous frequency of the associated electric field relative to the nearest cavity eigenfrequency (dashed line) for the single mode excitation of a 13.4 cm cavity (ν_f=1.12 GHz, $\mathscr{L}_{mn}$=0.002/pass) by a transform-limited Gaussian pulse ($\Delta\nu_{\mathrm{FWHM}}$=93 MHz, Δt_{FWHM}=4.80 ns). Note that the exponential decay of the ring-down signal only contains information about light at the cavity eigenfrequency.

In this expression, the integrand represents the power spectrum of the light exiting the cavity. For the case of perfect mode matching, when the cavity linewidth is small relative to the bandwidth of the input laser power spectrum, and when the cavity mode spacing is large relative to the input spectral bandwidth, Eq. (15) yields the intuitive result that measurement of the transmitted energy as a function of laser carrier frequency simply maps out the laser's power spectrum. In the opposite limit, when the laser's power spectrum is narrow compared to the cavity linewidth, this expression yields the familiar Fabry–Pérot intensity transmission function which is given by the square of the modulus of Eq. (9). When the width of the laser power spectrum becomes comparable to the cavity longitudinal mode spacing, adjacent transmission peaks start to overlap and modulation in the transmitted energy is reduced. In this regime, the transmittance becomes independent of the laser carrier frequency. However, this does not imply that all laser frequencies are transmitted by the cavity. On the contrary, Eq. (15) shows that only light at frequencies near the cavity eigenfrequencies contributes to the transmittance. Coupling into multiple transverse modes tends to reduce further any modulation in the transmittance. Finally, in their recent paper Zalicki and Zare[3] presented cavity transmittances calculated using a time-domain formalism and assuming excitation of a single transverse mode. Calculations using Eq. (15) and the excitation spectrum implied in their analysis yield results identical to theirs.

Since the cavity transmittance is measured on a time-averaged basis, there are several effects which could prevent the experimental realization of the transmittance predicted by Eq. (15). An obvious effect is shot-to-shot variations in the excitation power spectrum. Another mechanism is fluctuations in the cavity eigenfrequencies associated with changes in the optical pathlength. A change in the optical pathlength of δl will shift the cavity eigenfrequencies by[34]

$$\delta\omega\approx-\frac{\delta l}{\lambda/2}\cdot\omega_f. \tag{16}$$

When fluctuations in l associated with mechanical vibrations and thermal expansion of the cavity are slow relative to τ_{mn}, single-shot cavity linewidths may not be degraded.[35] Nevertheless, such fluctuations in the cavity optical pathlength can be important over the course of time-averaged measurements. Consequently, the narrow transmittance features predicted by Eq. (15) can only be realized with length-stabilized cavities. Similar effects can arise from density fluctuations in the cavity medium.

A useful model for the incident laser field that provides some insight into the effects of temporal incoherence on the ring-down signal is that of a Gaussian time envelope with a linear frequency modulation or chirp.[15] The model is useful because the time and frequency transform pairs of the field can be written in a closed form, and moreover it reflects the essential physics of the effect of temporal incoherence in the input field. This input field of amplitude E_0 can be written as

$$e_i(t) = E_0 \exp(-\gamma t^2 + i\beta t^2), \tag{17}$$

where β is the chirp parameter, and the instantaneous angular frequency is,

$$\omega(t) = \omega_c - 2\beta t. \tag{18}$$

The temporal duration of the intensity of the input laser pulse is

$$\Delta t_{\mathrm{FWHM}} = \sqrt{\frac{2\ln(2)}{\gamma}}, \tag{19}$$

and for this pulse the time-bandwidth product is

$$\Delta\omega_{\mathrm{FWHM}} \cdot \Delta t_{\mathrm{FWHM}} = 4\ln(2)\sqrt{1+(\beta/\gamma)^2}, \tag{20}$$

where the times-transform-limit factor, $n_t = \sqrt{1+(\beta/\gamma)^2}$, is the ratio of the bandwidth of the pulse to the bandwidth of a transform-limited pulse having the same temporal width. In the limit that $\beta \to 0$, Eq. (20) reduces to the well known reciprocity relation for transform-limited Gaussian pulses.

Subject to the same assumptions used in the derivation of Eq. (14) and assuming that the orthogonality of the transverse modes is preserved, excitation by a chirped Gaussian pulse leads to

$$\begin{aligned}\dot{\mathscr{E}}(t) = 2\sqrt{\epsilon_0/\mu_0}\,\frac{E_0^2\pi}{\sigma_{\mathrm{eff}}^2}\sum_{mn}|C_{mn}|^2\Bigg\{&\sum_{q=q_{\min}}^{q_{\max}}\Gamma_{mn}^2\exp(-(\omega_{qmn}-\omega_c)^2/2\sigma_{\mathrm{eff}}^2)\cdot\exp(-2\Gamma_{mn}t)\\ &+2\sum_{q=q_{\min}}^{q_{\max}-1}\sum_{q'=q+1}^{q_{\max}}\Gamma_{mn}^2\exp(-(\omega_{qmn}-\omega_c)^2/4\sigma_{\mathrm{eff}}^2)\cdot\exp(-(\omega_{q'mn}-\omega_c)^2/4\sigma_{\mathrm{eff}}^2)\cdot\exp(-2\Gamma_{mn}t)\\ &\cdot\cos[(\omega_{qmn}-\omega_{q'mn})t+\phi(\omega_{qmn}-\omega_c)-\phi(\omega_{q'mn}-\omega_c)]\Bigg\},\end{aligned} \tag{21}$$

for the output signal of the ring-down cavity, where, the effective $e^{-1/2}$ angular frequency half-width of the excitation power spectrum is

$$\sigma_{\mathrm{eff}} = \sqrt{\gamma[1+(\beta/\gamma)^2]} = n_t\sqrt{\gamma}, \tag{22}$$

and in which the spectral phase of the input field is

$$\phi_i(\omega-\omega_c) = \phi_0 + \frac{1}{2}\arctan\frac{\beta}{\gamma} - \frac{\beta(\omega-\omega_c)^2}{4(\gamma^2+\beta^2)}. \tag{23}$$

III. DISCUSSION

A. Mode beating effects

The number of longitudinal modes contributing to the signal scales with the ratio of twice the laser linewidth to the longitudinal mode spacing of the cavity, $\eta = 2\cdot\sigma_{\mathrm{eff}}/\omega_f$. Defining a "short" cavity as one for which $\eta \ll 1$, in this limit a single longitudinal mode for each transverse mode will be dominant, and the total energy transmitted by the cavity will vary strongly with ω_c. The excitation of a single mode will yield a single exponential decay, as long as orthogonality is maintained and losses are independent of transverse mode order. Consider next the opposite extreme, denoted as the "long" cavity limit where $\eta \gtrsim 1$. In this limit, several longitudinal modes will be excited regardless of ω_c and longitudinal mode beating will occur. For this case, $\dot{\mathscr{E}}(t)$ corresponds to a series of pulses separated in time by the cavity round-trip time where the pulse amplitudes are exponentially decaying. Given excitation of a single transverse mode, the envelope of $\dot{\mathscr{E}}(t)$ will be a single exponential having a decay constant characteristic of that transverse mode and neither the depth of modulation of the pulses nor the total energy transmitted by the cavity will depend greatly on ω_c. For the "intermediate" case in which the cavity is neither "short" nor "long," $\dot{\mathscr{E}}(t)$ will be a decaying signal modulated by longitudinal and perhaps transverse mode beats, with a modulation depth dependent on ω_c and η.

To illustrate these mode beating effects for the "short," "intermediate," and "long" cavity cases, Eq. (21) was used to model output signals, using transform-limited pulses with $\eta = 0.1$, 0.75, and 1.25. The results are shown in Fig. 2. In the case $\eta = 0.75$, although the modulation depth is sensitive to ω_c, this effect is diminished when multiple transverse modes are excited. Thus, to the extent that the excitation is not mode matched, variations in the modulation depth of the output pulses for cavities of "intermediate" length (as a consequence of shot-to-shot variations in ω_c) will be reduced. For the "long" cavity excitation [Fig. 2(c)] the shape of the output pulses is very nearly Gaussian and appears to be a replica of the input pulse. However, because of the frequency selectivity of the cavity, we reiterate that the power spectrum of the light exiting the cavity is not identical to the excitation power spectrum.

B. Coherence effects

As Wolf and co-workers[36,37] have demonstrated, the degree of coherence for any electromagnetic field in a cavity can be described using the fundamental cavity eigenmodes. Also, as demonstrated by Lehmann and Romanini,[10] incoherence in the excitation pulse in no way affects the frequency response of a cavity. Thus, the present eigenmode analysis of cavity excitation by nontransform limited pulses should properly account for the coherence of the incident field.

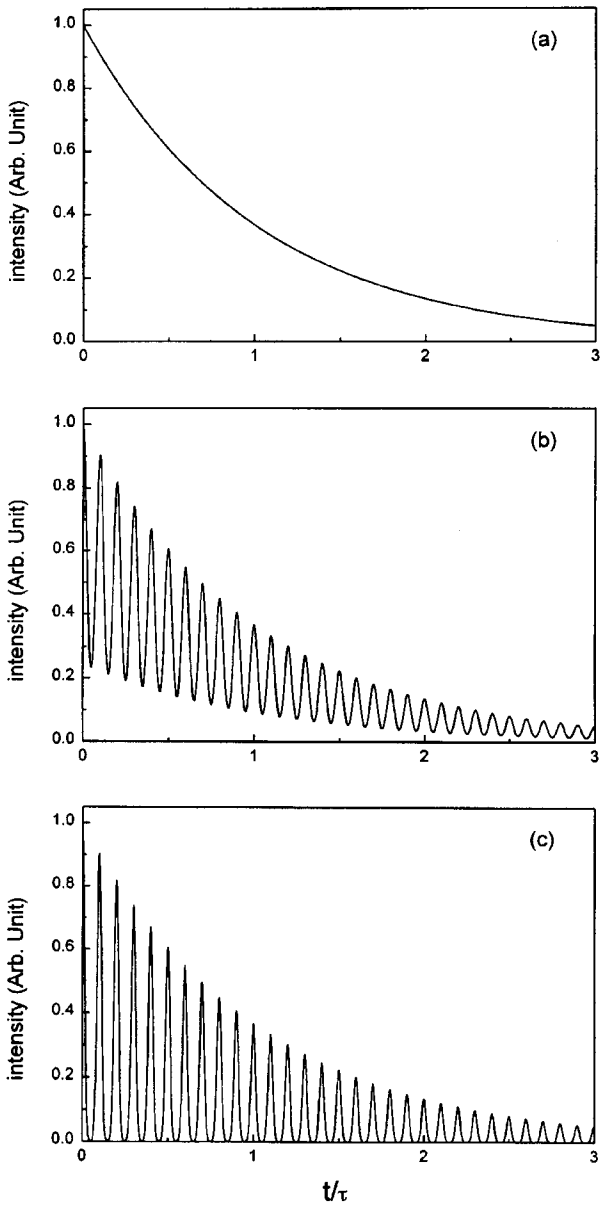

FIG. 2. Ring-down signals calculated using Eq. (21) for (a) "short," (b) "intermediate," and (c) "long" cavity cases for transform-limited pulses with η=0.1, 0.75, and 1.25, respectively. For these calculations, the excitation spectrum was centered on a cavity eigenfrequency.

To investigate further the role of temporal incoherence in the incident field, we have used Eq. (21) to calculate ring-down signals for chirped pulses. In Fig. 3 we present a portion of the output signal of a 100 cm long cavity for excitation by three different pulses having the same energy. These cases are labeled (a), (b), and (c) and correspond to $(\Delta t_{\mathrm{FWHM}}, \Delta\nu_{\mathrm{FWHM}}, n_t)$=(3.30 ns, 134 MHz, 1), (3.30 ns, 535 MHz, 4) and (0.825 ns, 535 MHz, 1), respectively. The excitations associated with cases (a) and (b) have the same temporal envelopes, whereas those of cases (b) and (c) have equivalent bandwidths. The total energy transmitted for case

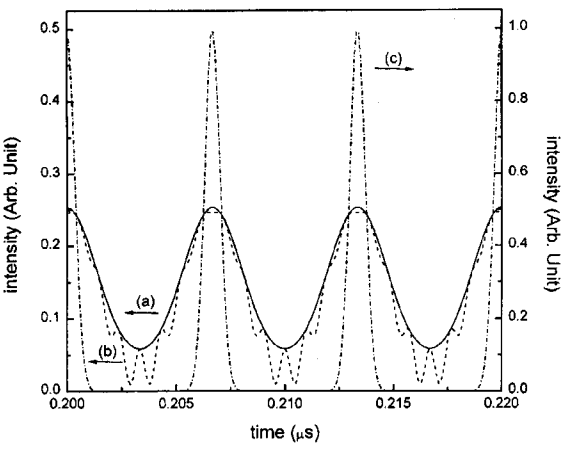

FIG. 3. A portion of the ring-down signal calculated using Eq. (21) for a 100 cm cavity for excitation by three pulses having the same energy but with varying bandwidth and temporal coherence. The three cases are labeled (a), (b), and (c) and correspond to $(\Delta t_{\mathrm{FWHM}}, \Delta\nu_{\mathrm{FWHM}}, n_t)$=(3.30 ns, 134 MHz, 1), (3.30 ns, 535 MHz, 4) and (0.825 ns, 535 MHz, 1), respectively. The excitations associated with cases (a) and (b) have the same temporal envelopes, whereas those of cases (b) and (c) have equivalent bandwidths.

(b) is approximately 10% less than that of case (a), while cases (b) and (c) are predicted to have identical throughputs. Turning to Fig. 3, the time-integrated signals corresponding to cases (a), (b), and (c) give the same relative energy transmittance as predicted by Eq. (15). Comparison of cases (a) and (b) shows that the main effect of the chirp in the excitation is to distort the emergent pulses. Comparison of case (b) to case (c) also indicates that chirp in the excitation yields distorted pulses at the cavity exit. These calculations reveal that the changes in the temporal coherence associated with different degrees of chirp in the excitation are encoded in the $\phi_i(\omega-\omega_c)$ and manifest primarily in the shape of the pulses exiting the cavity. For "short" cavities and in the limit that the excitation phase does not vary significantly over the cavity linewidth, the purely exponential ring-down signal will be essentially independent of the temporal coherence of the laser pulse. Also, since ring-down signals depend on the incident pulse's coherence, we speculate that "intermediate" length ring-down cavities may be used as a tool for the characterization of incoherence in laser pulses.

Scherer *et al.*[6,9] have recently discussed the frequency response of ring-down cavities to excitation by pulses of varying coherence properties. They asserted that the frequency selectivity of the cavity depends largely on the ratio of the round-trip cavity length, $2\cdot l$, to the coherence length, l_c, of the input laser pulse. According to their analysis, for $2\cdot l/l_c \gtrsim 1$, ring-down cavities are not frequency selective, and it is claimed that experimental measurements of constant transmittance as a function of laser carrier frequency support this model. Conversely, they claimed that ring-down cavities exhibit frequency selectivity only in the regime, $2\cdot l/l_c \lesssim 1$. Their results are at odds with the present analysis.

We would like to offer a few comments on their analysis, particularly on the use of coherence length to predict the

transmittance properties of ring-down cavities. First, it is well known that the response function for a linear optical device depends only on system parameters (e.g., mirror reflectivities, geometry) and not on the incident field.[15,38] Second, the coherence time, $\tau_c = l_c/c$ can be defined in a number of ways,[39] and as such it provides neither a unique nor complete measure of the degree of temporal coherence of a laser pulse. As an example, Wolf has defined τ_c as the normalized root-mean-square width of the autocorrelation of the complex analytic field amplitude at a given point in space while Mandel has defined τ_c to be the power-equivalent width of the normalized autocorrelation function. For pulses with Gaussian temporal and spectral distributions, Wolf's definition gives, $\tau_c = \Delta t_{\mathrm{FWHM}}/(2\sqrt{\ln(2)})$, while that of Mandel is strictly proportional to the reciprocal of the spectral width, $\tau_c = \Delta\omega_{\mathrm{FWHM}}^{-1}\sqrt{8\ln(2)\pi}$. Thus, by the first definition, cases (a) and (b) considered above have the same coherence lengths, whereas in terms of the second definition, the coherence lengths of cases (b) and (c) are identical. We conclude that the use of coherence time of the excitation pulse cannot be used to predict cavity response. Rather, when addressing coherence effects, the cavity response function and a rigorous description of the excitation field, $a_i(\omega-\omega_c)$ and $\phi_i(\omega-\omega_c)$, are required.

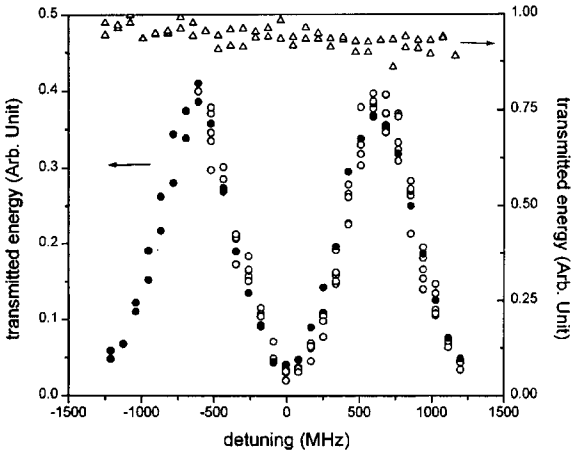

FIG. 4. The measured transmitted energy at the exit of a ring down cavity, $\mathscr{E}$, as a function of laser frequency for a nonlength-stabilized degenerate cavity (magic number equal to 6), excited with a single-mode pulsed laser (~100 MHz FWHM). The data taken with an intracavity aperture present exhibit a strong modulation in the cavity transmittance with laser frequency. These data are indicated by ○ and ● for scanning of the laser frequency in positive and negative directions, respectively. The data taken with an intracavity aperture removed, indicated by △, exhibit no modulation with laser frequency.

IV. EXPERIMENT

To test certain conclusions of the foregoing analysis, we have carried out two sets of experiments. In the first set of experiments, we demonstrate that the transmittance of a cavity modulates as a function of laser detuning, as implied by Eq. (15). In the second set of experiments we show that the observed ring-down signals can be understood in terms of cavity mode beating for all cavity lengths investigated, as implied by Eq. (14).

The cavities were constructed from 2.54 cm diameter, 100 cm radius of curvature mirrors with maximum reflectivity, $R \sim 0.9998$ near 810 nm. The mirrors were held in good quality mirror mounts that were mounted on 2.54 cm diameter stainless steel mounting posts bolted to an optical table. The cavities were open to room air and no particular effort was taken to stabilize the cavity length. The ring-down signals were measured with a low gain photomultiplier tube terminated into 50 Ω and digitized with an 8 bit, 1 GSample/s digitizing oscilloscope. The rise time of this detection system is estimated to be better than 1 ns.

In the first set of experiments, we report transmittance measurements of a 13.39 cm open air cavity. For this cavity, the longitudinal mode spacing is 1.12 GHz and adjacent transverse modes are separated by one sixth the longitudinal mode spacing (187 MHz). The cavity was injected with light from a pulsed Nd^{3+}:YAG-pumped dye cell amplifier chain that was seeded by a single-mode, tunable continuous wave diode laser. The resulting pulse had a nearly Gaussian time profile with ~4.8 ns FWHM, and its single-shot spectrum was determined to be ~100 MHz FWHM at a nominal wavelength of 840 nm. The beam was shaped with a simple Galilean telescope, and at the input mirror the beam profile was approximately rectangular of nominal dimensions 1 mm×3 mm. No particular effort was made to mode match into this cavity.

The excitation of high order transverse modes was suppressed by placing a 1.5 mm intracavity aperture (approximately three times the TEM_{00} e^{-1} waist diameter) at the center of the cavity. The effective Fresnel number[40] for this cavity is ~20. At a given laser carrier frequency, the ring-down signal was integrated over an ~20 μs time window (>5 e^{-1} ring-down time constants) beginning near $t=0$ for each laser shot, and 500 or more shots were averaged together to give a measure of the transmitted energy. The signals were not normalized for variations in the laser energy.

Figure 4 displays the time-averaged (multishot) transmitted energy with laser detuning for this cavity. Clearly evident in this figure is a deep modulation, and the maxima are separated by 1.12 GHz, which corresponds to the calculated free spectral range of the cavity. The FWHM of the features is ~540 MHz. At the peak of the transmittance, the single shot ring-down signals were exponential with a time constant of ~3.5 μs, corresponding to intracavity losses of $\sim 1.25\times 10^{-4}$/pass. The transmittance curve in Fig. 4 was recorded by tuning the laser from low to high frequency and then from high to low frequency. Tuning the laser in either direction gave the same result.

The successful coupling into low order modes was confirmed by monitoring the intensity profile of the light emerging from the end of the cavity opposite injection with a CCD camera. At a transmittance maximum, the intensity profile was observed to be usually a TEM_{00}, sometimes a TEM_{01}, and rarely some more complicated transverse mode. The TEM_{00} or TEM_{01} profiles were fit with the Gauss–Hermite

wave functions and gave a best-fit Gaussian beam e^{-1} diameter of 0.522 mm. This value is within 3% of the calculated diameter of 0.536 mm for this cavity. When the laser was tuned off resonance, in contrast, most shots had no measurable intensity. Those that did usually displayed some high order, more complicated transverse mode pattern with peak intensities much less than the profiles observed on resonance.

The transmittance was measured again in a second experiment with the same cavity without the intracavity aperture. This data, also shown in Fig. 4, clearly lack the structure so readily apparent when the aperture was in place. The slight slope in the transmittance is probably an artifact of the uncompensated drift in the laser pulse energy. The intensity profiles were highly structured, did not correspond to simple cavity modes, and varied from shot-to-shot, indicating the excitation of relatively high order transverse modes.

For excitation of a single transverse mode, Eq. (15) predicts that the linewidth of an isolated resonance is given by the convolution of the laser power spectrum with the Fabry–Perot transmission function. The cavity linewidth, inferred from the measured ring-down time constant, is ~45 kHz and is negligible in comparison to the single-shot laser bandwidth of ~100 MHz. The predicted linewidth is therefore much smaller than the measured value of 540 MHz for the intracavity aperture case. The disparity between the measured linewidths and the model prediction can be attributed to frequency jitter in the excitation laser, the effects of mechanical instabilities, and density fluctuations, as discussed earlier. A change in cavity length of only 100 nm is sufficient to shift the cavity transmittance peak by some 300 MHz. Similarly, a change in the pressure of 100 Pa (0.75 Torr) would shift the transmittance peak by approximately 100 MHz. Changes of these magnitudes are reasonable, given the construction of this cavity. As given by Eq. (15), for multimode excitation, the transmittance is a sum of the transmittances associated with the individual transverse modes. The superposition of six transmittance curves, separated by 187 MHz, and each having a FWHM of 540 MHz, would give a constant transmittance, consistent with the no-aperture data presented in Fig. 4.

Scherer *et al.*[9] reported a set of experiments from which they concluded that there is no frequency selectivity for pulsed excitation of a "short" ring-down cavity. This conclusion was drawn from two experimental results: the observation of a constant transmittance for "short" unstabilized cavities, and the observation of all anticipated features in CRD absorption spectra. These results can be interpreted in the context of our model. As discussed above, observation of a constant transmittance does not imply that the cavity is not frequency selective. Imperfect mode matching or misalignment of the input beam could have excited multiple transverse modes, and since Scherer *et al.*[9] used nondegenerate cavities there was a virtual continuum[18] of modes in which to couple. These effects were doubtlessly exacerbated by the use of unstabilized cavities and frequency jitter in their excitation laser.

In the second set of experiments we test our interpretation of ring-down signals in terms of longitudinal and transverse mode beating using "short," "intermediate," and "long" cavities. The observation of transverse mode beating, which can be observed by destroying the orthogonality[41,42] of the transverse modes, is considered to be "a subtle but very significant confirmation of the (stable resonator) theory." [43] For the "short," magic number six cavity, described above, all transverse modes would be expected to beat at multiples of the fundamental transverse mode spacing, 187 MHz. By slightly misaligning the cavity to promote off-axis injection of the laser beam and to destroy the orthogonality of the transverse modes, ring-down signals dominated by transverse mode beating were obtained. A typical signal for this case, shown in Fig. 5, appears as an exponential decay with a deep sinusoidal modulation. In the inset of Fig. 5, a limited range of the data is fit very closely by a sinusoid at the predicted fundamental frequency of 187 MHz. For this case, no other beat frequencies were observed.

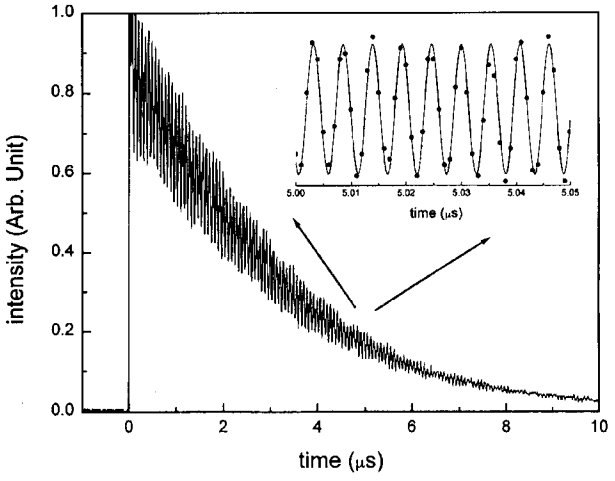

FIG. 5. The ring-down signal measured for a magic number 6 cavity (identical to the cavity used to record the data in Fig. 4) which displays clear evidence of transverse mode beating. In this case, the cavity was slightly misaligned to destroy the orthogonality of the transverse modes. The decay time constant, which is 3.5 μs, corresponds to a nominal loss of 125×10^{-6} per pass and mode linewidth of 45 kHz. Note that in the main figure, due to undersampling in the data display, aliasing effects give the false impression of a low frequency beat signal. Inspection of the inset, however, reveals that measured modulation, (●), is well described by a sinusoid (solid line) at the transverse mode spacing of 187 MHz.

Experiments were carried out to look at both longitudinal and transverse mode beating in two "intermediate" length magic number cavities. In these experiments, the light source was a Littman-oscillator-based Ti:Al_2O_3 laser pumped by a Nd^{3+}:YAG laser. The single-shot laser output from was a near-transform-limited pulse, having a FWHM of ~3.3 ns, giving an estimated bandwidth of ~135 MHz FWHM near 760 nm. As with the cavity above, intracavity apertures and a CCD camera were used to ensure on-axis beam propagation and proper alignment of the cavity. We examined a 29.3 cm cavity (where ν_f=512 MHz and ν_f/ν_{tr}=4), and a 100 cm cavity (in which ν_f=150 MHz and ν_f/ν_{tr}=2). Transverse mode beating was induced by placing a small strip of paper in front of the photomultiplier. For

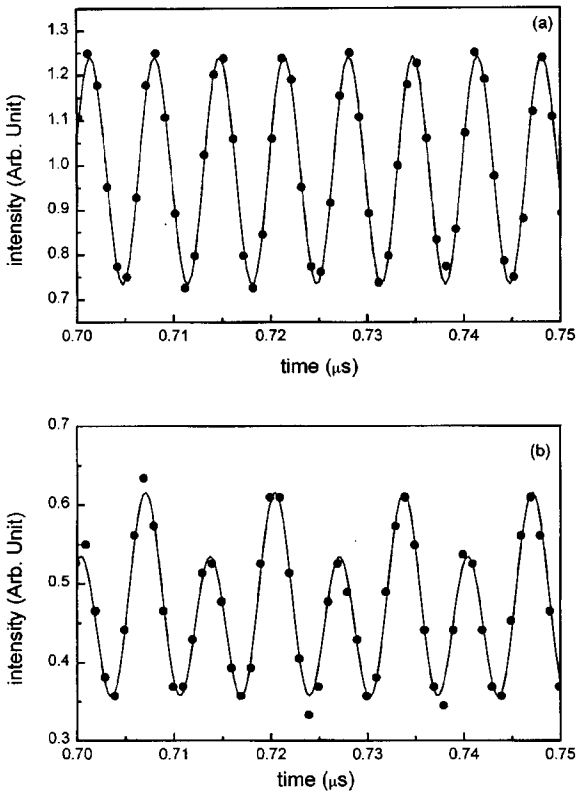

FIG. 6. A portion of a measured (●) ring-down signal providing evidence of longitudinal and transverse mode heating in a confocal cavity when the detector was (a) unobscured and (b) partially blocked. The solid lines in both figures represent best-fit sine waves with beat frequencies of 150 MHz and 75 MHz. In (a), only beating at the longitudinal mode spacing, $\nu_f = 150$ MHz is evident, whereas in (b) frequencies at both the longitudinal and transverse mode spacings of 150 MHz and 75 MHz, respectively, are observed.

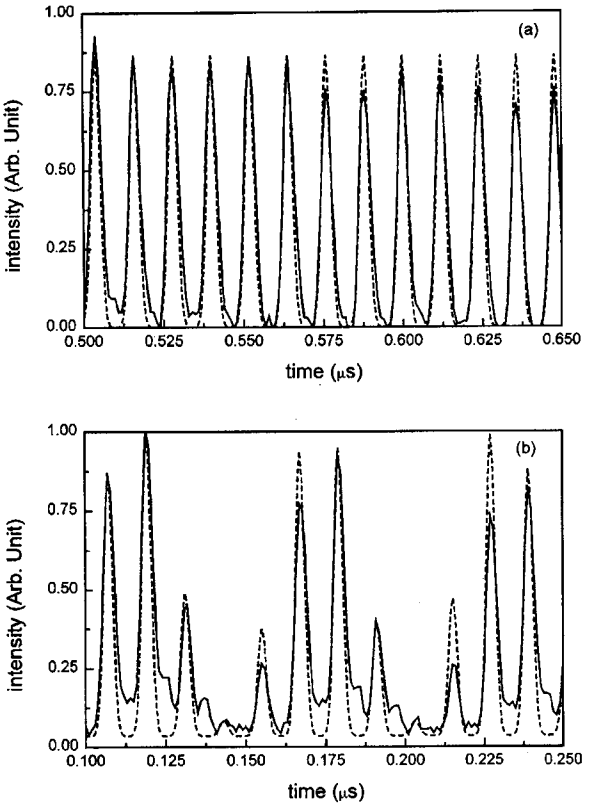

FIG. 7. A portion of a measured ring-down signal (solid line) providing evidence of longitudinal and transverse mode beating in "long" nondegenerate cavity when the detector was (a) unobscured and (b) partially blocked. Here, the cavity length $l = 180$ cm and the round-trip time $t_r = 12$ ns and the cavity was excited by a transform-limited pulse having an intensity FWHM of 3.25 ns. In both figures, the measurements compare favorably to model simulations (dashed lines), which are discussed in the text. In (a), the output signal is well described by longitudinal mode beating simulation using Eq. (24). In this case, the temporal envelopes of the pulses exiting the cavity are very nearly Gaussian and are separated by t_r. In (b), partial obscuration of the detector gives rise to a very complicated output signal. This output is quasi-periodic with a frequency of ~17 MHz which corresponds to the difference between the longitudinal and transverse mode spacings. In the simulation of this signal, Eq. (23) was used and two transverse modes, separated by $\Delta(m+n) = 1$, were assumed to dominate the response.

these cavities, we observed very strong mode beating at multiples of the transverse mode spacing equal to 128 MHz and 75 MHz, respectively. As shown in Fig. 6, without blocking the detector, longitudinal mode beating at 150 MHz was observed for the 100 cm cavity, and when the detector was partially obscured, clear beats at 75 MHz arose. The solid curve shown in Fig. 6(b), a least squares fit based on a linear combination of 75 MHz and 150 MHz sinusoidal beats, matches the measurements.

To look for evidence of modes in "long" ring-down cavities, we looked for evidence of mode beating using a 180 cm cavity. For this nondegenerate cavity, ν_f and ν_{tr} were 83.4 MHz and 66.1 MHz, respectively. Figure 7 shows two ring-down signals measured using this cavity and the Littman-oscillator-based Ti:Al_2O_3 laser. With the detector unobscured, a succession of damped pulses, separated by the round-trip time of 12 ns was observed [Fig. 7(a)]. Superimposed on the data is a ring-down signal, calculated using Eq. (21), where we have assumed a transform-limited pulse with $\Delta\nu_{\mathrm{FWHM}} = 135$ MHz. Data obtained for this cavity with the detector partially blocked [Fig. 7(b)] show clear evidence of transverse mode beating effects. The detailed shape of the ring-down signal depends on what portion of the beam was blocked. Inspection of Fig. 7(b) reveals a complicated yet nearly periodic waveform having a frequency of ~17 MHz, a frequency that corresponds to the difference between the longitudinal and transverse mode spacings. Also shown in Fig. 7(b) is a calculated ring-down signal based on Eq. (14). For this computation, beating between a pair of transverse modes separated by $\Delta(m+n) = 1$ was assumed, and the amount of coupling into each of these modes, as well as the degree of nonorthogonality between the modes, were adjusted to give a good representation of the data. Given the number of parameters in the model, nonidealities in the laser and photomultiplier response and the complicated temporal structure of the signal, agreement between the model and experiment is quite good.

The observations of mode beating in the all cavities at the predicted frequencies, coupled with observations of the TEM_{00} and TEM_{01} eigenmodes for the "short" magic number six cavity, demonstrate the existence of transverse and longitudinal modes within empty ring-down cavities. These measurements also demonstrate that even when the cavity is "long" the observed signals are still interpretable in terms of the cavity mode structure and stable resonator theory.

V. CONCLUSIONS

In this paper we have presented an analysis of the time and frequency dependence of the signals observed with empty cavities based on stable resonator theory. Many predictions of this analysis were experimentally verified. From this analysis, we conclude that regardless of the cavity length, ring-down cavities sustain well-defined modes and are therefore inherently frequently selective. However, when considering time-averaged data, mode effects may be obfuscated by the use of unstabilized cavities or poor mode matching. Thus, as discussed by Zalicki and Zare,[3] spectral distortion could result and caution may be necessary in interpreting ring-down spectra.

Although we have focused on the response of ring-down cavities under pulsed excitation, the analysis presented here is by no means limited to this special case. The response of a cavity to modulated continuous-wave laser beams can also be analyzed with this formalism.[44] Similarly excitation by a multimode laser can be incorporated into the present analysis by superposing a set of pulses, with each pulse having a unique phase, $\phi^{(j)}$ and carrier frequency, $\omega_c^{(j)}$, to yield the total excitation field, $\Sigma_j e_i^{(j)}(t)$.

Depending on the application, there are several possible approaches which may be taken in the design and implementation of a CRDS-based system. We identify at least three generic applications having different optimal configurations. First, for general-purpose spectroscopic measurements requiring only moderate frequency resolution,[45–48] the use of "long," nonstabilized and nondegenerate, large-aperture cavities may be appropriate. With this approach, mode effects would be averaged out and all spectral features would be observable as the probe laser is scanned. In this case, quantitative CRDS absorption measurements are possible when laser bandwidth effects are accounted for properly. Second is the case of quantitative, high sensitivity absorbance measurements.[7,8] Here one would wish to achieve the shot noise limit, which may not be possible due to quasirandom, shot-to-shot variations in transverse mode beats. In this case, one should use nearly degenerate, "short" cavities, which should allow one to filter out transverse mode beating. Since maximum sensitivity is achieved with long path lengths, one must design the system so that the "short" cavity criterion is satisfied. Third, as cleverly pointed out by Lehmann and Romanini,[10] one might design experiments to fully exploit the very high frequency resolution inherent in ring-down cavities.[49] In principle, one could obtain very high resolution spectra with broadband laser sources if the cavities are length stabilized. We would like to add that this approach would also be realized best by building relatively short, degenerate cavities. Such a configuration would result in the excitation of a family of degenerate modes all about a single frequency, thus relaxing the stringent demands on transverse mode matching into the cavity which would be otherwise be required.

In order that the potential of cavity ring-down spectroscopy be fully exploited, it is undoubtedly important that the practitioners of CRDS consider the underlying physical principles. It is in this context that we have offered the foregoing analysis. To those already experienced with the technique, this exposition might clarify any ambiguities which may have existed. To the new users of CRDS, we hope that this work will complement the existing body of literature on the subject and perhaps help to motivate future investigations.

Note added in proof. Subsequent to submission of this manuscript, Zare and co-workers have reported experiments and an analysis comparable to and in good agreement with the findings reported here [J. Martin, B. A. Paldus, P. Zalicki, E. H. Wahl, T. G. Owano, J. S. Harris, Jr., C. H. Kruger, and R. N. Zare, Chem. Phys. Lett. **258**, 63 (1996); J. Martin and R. N. Zare (private communication)].

ACKNOWLEDGMENTS

We thank Dr. S. Bergeson for use of the laser system used in for the cavity transmittance measurements. We also are grateful to Professor K. K. Lehmann, Professor J. A. Lock, Dr. G. J. Rosasco, and Professor R. N. Zare for many helpful discussions and to Dr. A. O'Keefe and Dr. J. J. Scherer for a candid discussion of their experimental system.

[1] A. O'Keefe and D. A. G. Deacon, Rev. Sci. Instrum. **59**, 2544 (1988).
[2] D. Romanini and K. K. Lehmann, J. Chem. Phys. **99**, 6287 (1993).
[3] P. Zalicki and R. N. Zare, J. Chem. Phys. **102**, 2708 (1995).
[4] J. R. Christian and G. Goubau, IRE Trans. Antennas Propog. **9**, 256 (1961).
[5] J. J. Scherer, J. B. Paul, C. P. Collier, and R. J. Saykally, J. Chem. Phys. **102**, 5190 (1995).
[6] J. J. Scherer, J. B. Paul, A. O'Keefe, and R. J. Saykally, in *Advances in Metal and Semiconductor Clusters*, Vol. 3, edited by M. A. Duncan (JAI, Greenwich, CT, 1995), p. 149.
[7] R. T. Jongma, M. G. H. Boogaarts, I. Holleman, and G. Meijer, Rev. Sci. Instrum. **66**, 2821 (1995).
[8] J. T. Hodges, J. P. Looney, and R. D. van Zee, Appl. Opt. **35**, 4112 (1996).
[9] J. J. Scherer, D. Voelkel, D. J. Rakestraw, J. B. Paul, C. P. Collier, R. J. Saykally, and A. O'Keefe, Chem. Phys. Lett. **245**, 273 (1995).
[10] K. K. Lehmann and D. Romanini, J. Chem. Phys. **105**, 10263 (1996), preceding paper.
[11] A. G. Fox and T. Li, Bell Syst. Tech. J. **40**, 453 (1961).
[12] G. D. Boyd and J. P. Gordon, Bell Syst. Tech. J. **40**, 489 (1961).
[13] H. Kogelnik and T. Li., Proc. IEEE **54**, 1312 (1966).
[14] L. Mandel and E. Wolf, *Optical Coherence and Quantum Optics* (Cambridge University Press, Cambridge, England, 1995), Chap. 3.
[15] J-C. Diels and W. Rudolph, *Ultrashort Laser Pulse Phenomena* (Academic, San Diego, CA, 1996), Chap. 1.
[16] G. D. Boyd and H. Kogelnik, Bell Syst. Tech. J. **41**, 1347 (1962).
[17] D. Herriot, H. Kogelnik, and R. Kompfner, Appl. Opt. **3**, 523 (1964).
[18] G. Meijer, M. G. H. Boogaarts, R. T. Jongma, D. H. Parker, and A. M. Wodtke, Chem. Phys. Lett. **217**, 112 (1994).
[19] A. E. Siegman, *Lasers* (University Science Books, Mills Valley, CA, 1986), p. 642 ff.
[20] H. Kogelnik, in *Proceedings of the Symposium on Quasi-Optics*, Microwave Research Institute Symposia Series **14**, 333 (1964).

[21] H. Boersch, H. Eichler, and G. Herziger, Phys. Lett. **11**, 291 (1964).
[22] F. Bayer-Helms, Appl. Opt. **23**, 1369 (1984).
[23] M. Born and E. Wolf, *Principles of Optics*, 6th ed. (Pergamon, Oxford, England, 1980), p. 325.
[24] F. Bayer-Helms, Z. Angew. Phys. **15**, 330 (1963).
[25] G. Koppelmann, in *Progress in Optics*, edited by E. Wolf (Wiley, New York, 1969), Vol. VII.
[26] A. E. Siegman, in Ref. 19, p. 770.
[27] D. Slepian, Bell. Sys. Tech. J. **44**, 3009 (1964).
[28] D. Slepian, J. Math. Phys. (MIT) **44**, 99 (1965).
[29] J. L. Remo, J. Opt. Soc. Am. B **8**, 1174 (1991).
[30] J. L. Remo, Appl. Opt. **20**, 2997 (1981).
[31] W. H. Steier, Appl. Opt. **5**, 1229 (1965).
[32] D. H. Auston, IEEE J. Quantum Electron. **4**, 420 (1968).
[33] P. W. Smith, Proc. IEEE **58**, 1342 (1970).
[34] A. E. Siegman, in Ref. 19, p. 437.
[35] K. An, C. Yang, R. R. Dasari, and M. S. Feld, Opt. Lett. **20**, 1068 (1995).
[36] E. Wolf and G. S. Agarwal, J. Opt. Soc. Am. A **1**, 541 (1984).
[37] L. Mandel and E. Wolf, in Ref. 14, p. 389 ff.
[38] E. Wolf and J. R. Fienup, Opt. Commun. **82**, 209 (1991).
[39] L. Mandel and E. Wolf, in Ref. 14, p. 179 ff.
[40] T. Li, Bell Syst. Tech. J. **42**, 2609 (1963).
[41] D. Rosenberger, Arch. Elektrischen. Ubertragung **17**, 202 (1963).
[42] J. P. Goldsborough, Appl. Opt. **3**, 267 (1964).
[43] A. E. Siegman, in Ref. 19, p. 773.
[44] D. Hils and J. L. Hall, Rev. Sci. Instrum. **58**, 1406 (1987).
[45] T. Yu and M. C. Lin, J. Am. Chem. Soc. **115**, 4371 (1993).
[46] D. Romanini and K. K. Lehmann, J. Chem. Phys. **102**, 633 (1995).
[47] P. Zalicki, Y. Ma, R. N. Zare, E. H. Wahl, J. R. Dadamio, T. G. Owano, and C. H. Kruger, Chem. Phys. Lett. **234**, 269 (1995).
[48] J. B. Paul, J. J. Scherer, C. P. Collier, and R. J. Saykally, J. Chem. Phys. **104**, 2782 (1996).
[49] R. Teets, J. Echstein, and T. W. Hansch, Phys. Rev. Lett. **38**, 760 (1977).